







Prediction Model With Harmonic Load Current Components for FCS-MPC of an Uninterruptible Power Supply

Sergio Vazquez , *Fellow, IEEE*, Eduardo Zafra , *Graduate Student Member, IEEE*,
Ricardo P. Aguilera , *Member, IEEE*, Tobias Geyer , *Senior Member, IEEE*,
Jose I. Leon , *Fellow, IEEE*, and Leopoldo G. Franquelo , *Life Fellow, IEEE*

Abstract—A finite control set model predictive control (FCS-MPC) strategy consists of a prediction model, a cost function and an optimization algorithm. Consequently, the performance of the FCS-MPC depends on the proper design of these three elements. This article assesses the influence of the prediction model of an uninterruptible power supply (UPS). Since the load connected to the voltage source inverter (VSI) affects the dynamic of the system state variables, the load dynamic should be included in the system model. This makes the design of the prediction model a challenge because the load connected to the VSI is generally unknown. To deal with this uncertainty, this work proposes an augmented prediction model based on a state observer that includes as many harmonic components as necessary to accurately represent the output current. The performance of the FCS-MPC for a UPS is evaluated in a laboratory prototype using the proposed and the conventional prediction models. Experimental results show that the proposed solution provides a more accurate representation of the output current, improving the system performance.

Index Terms—DC-AC power converters, Kalman filters, predictive control.

I. INTRODUCTION

FINITE control set model predictive control (FCS-MPC) is a powerful control strategy that has extensively been applied to power converters and drives in the last years [1]–[3]. This technique is considered as an advanced control strategy that provides several benefits compared to conventional solutions [4]. One of the main reasons for the success of the FCS-MPC is that the basics of the technique are easy to understand. This allows one to do an intuitive FCS-MPC design for any power conversion application [2]. In general, the designed FCS-MPC will be robust enough and provide a better system performance compared to conventional solutions even if the design criteria used are not the best [5], [6].

An FCS-MPC algorithm consists of a prediction model, a cost function and an optimization algorithm. The performance of a system governed by an FCS-MPC algorithm depends on the selected cost function, which defines the control targets, the accuracy of the prediction model to compute the future state variable values, and the ability of the optimization algorithm to compute the optimal control input within a sampling period.

The cost function is related to the particular application under consideration. Therefore, each application will use the most appropriate cost function to define the desired behavior of the state variables of interest. The cost function is composed of several terms associated with the tracking error of these state variables. A single cost function is required to control them simultaneously. Therefore, weighting factors are used to determine the relative importance of each control target [6], [7]. The design of the most suitable cost function has been investigated for many applications like motor drives, active front ends, uninterruptible power supplies (UPSs), etc., [2], [3], [8].

The optimization algorithm does not depend on the particular application, but determines the computational burden of the FCS-MPC algorithm. The computational cost is mainly determined by the length of the prediction horizon N_p used in FCS-MPC formulation. The prediction horizon determines the number of time steps the evolution of the state variables of interest is forecast into the future [9]. In general, long prediction horizons improve the system performance [6], [9]. The most common optimization algorithm is the exhaustive searching algorithm (ESA). The ESA evaluates the cost function for all

Manuscript received January 19, 2021; revised June 2, 2021; accepted July 15, 2021. Date of publication July 26, 2021; date of current version September 16, 2021. This work was supported in part by the Horizon 2020 Spartan Project under Grant 821381, in part by the Consejería de Economía, Conocimiento, Empresas, y Universidad, Secretaría General de Universidades, Investigación y Tecnología, under Project P18-RT-1340, and in part by the Australian Government through the Australian Research Council under Discovery Project DP210101382. The work of Eduardo Zafra was supported by the Spanish Ministry of Universities under Grant FPU18/02704. Recommended for publication by Associate Editor J. Rodriguez. (Corresponding author: Sergio Vazquez.)

Sergio Vazquez is with the Laboratory of Engineering for Energy, Environmental Sustainability, Universidad de Sevilla, C.P. 41092 Sevilla, Spain (e-mail: sergi@us.es).

Eduardo Zafra is with the Electronics Department, Universidad de Sevilla 41092 Sevilla, Spain (e-mail: ezafral@us.es).

Ricardo P. Aguilera is with the School of Electrical, Data Engineering, University of Technology Sydney, Sydney, NSW 2007, Australia (e-mail: raguilera@ieee.org).

Tobias Geyer is with the ABB System Drives, 5300 Turgi, Switzerland (e-mail: t.geyer@ieee.org).

Jose I. Leon and Leopoldo G. Franquelo are with the Laboratory of Engineering for Energy, Environmental Sustainability, Universidad de Sevilla 41092 Sevilla, Spain, and also with the School of Astronautics, Harbin Institute of Technology, Harbin 150001, China (e-mail: jileon@gte.esi.us.es; lgfranquelo@ieee.org).

Color versions of one or more figures in this article are available at <https://doi.org/10.1109/TPEL.2021.3098948>.

Digital Object Identifier 10.1109/TPEL.2021.3098948

the elements in the input control set. Then, it determines by direct comparison the one that minimizes the cost function. Considering the current development of digital control hardware platforms, this approach is suitable for short prediction horizons $N_p \in \{1, 2\}$, [10]. However, a different strategy is necessary for long prediction horizons $N_p \geq 3$ because the ESA is not computational feasible for such N_p in a practical application. Solutions for dealing with this problem draw on branch and bound techniques to reduce the computational burden [11]. Among them, the sphere decoding algorithm (SDA) is a suitable solution for a practical implementation [12], [13].

The prediction model is formed by the dynamic equation of the state variables of interest. For a power conversion system, it relies on the electric circuit connected to the output of the power converter. As a consequence, it depends on the particular application. In general, it is possible to have an accurate prediction model for power conversion systems like motor drives or active front ends. The dynamic equations of the state variables for the former are related to the kind of machine [14]–[18], whereas for the latter they depend on the connection filter [19]–[22]. A common approach to deal with parameter uncertainty problems in the prediction model is the use of observer-based techniques [23]–[27]. A different approach is the model-free predictive control that make predictions of the state variable future values without using a system model. In the literature two alternatives exist. On the one hand, a system identification method, like artificial neural networks (ANN), recursive least squares (RLS) algorithm, or ultralocal model, are used to define the system behavior. Once the system is identified, this information replaces the original system model to compute the state variable future values [28]–[30]. On the other hand, a different approach uses the system properties assuming a fast sampling period for the FCS-MPC to make the predictions of the state variable future values without using any model [31]–[33]. Although these techniques are promising, up to the authors knowledge, they have not been applied to an UPS application yet, so further research is required.

In general, model-free methods are good approaches when little or no information about the system is available. In the UPS application case, the system behavior is well represented by the output filter dynamic equations and the output load behavior. Compared to the model-free strategies, this work proposes an observer-based approach that exploits an explicitly given mathematical model of the system providing a simple and straightforward implementation.

This article focuses on the prediction model of FCS-MPC for a UPS application. The definition of this prediction model is challenging because the output load connected to the power converter is unknown. However, the dynamic equations of the state variables depend on the output load currents. Therefore, to solve this issue, it is necessary to make some assumptions about the current load behavior, which will affect the performance of FCS-MPC. The most common approach to deal with this uncertainty is to assume that the output load current remains constant between two consecutive sampling steps [34]. This assumption relies on the high sampling frequency typically used for FCS-MPC and generally provides acceptable results. To

implement this solution, the output load current can be measured, [35] or an observer can be designed to deal with system uncertainties and avoid additional sensors [34], [36].

A more precise solution is to model the characteristics of the load connected to the power converter [37]. This method provides an accurate representation of the load since no assumption about the load behavior is considered. However, in the literature this option is limited to linear loads for UPS systems [38], and for estimating the harmonics under distorted grid voltage for a grid-connected application [39]. An alternative solution is to adopt the constant load current approach and to modify the cost function to take into account the error introduced by the prediction model [40]. This procedure provides good results, especially when nonlinear loads are connected to the power converter. However, it increases the complexity of the cost function design.

The work at hands proposes a solution that takes into account that the load current is a periodical signal, independently whether the load is linear or not. Therefore, the load current can be decomposed by the sum of several harmonic components. More specifically, it is proposed to design the prediction model by using an augmented state observer that includes as many harmonic components as necessary to accurately represent the output current. This avoids the use of extra sensors, and allows the prediction model to deal with system uncertainties and any kind of output load. The augmented state observer is designed as a stationary Kalman filter. In contrast to [39], this work provide guidelines to set the values of the Kalman filter matrices, which is of high value for practical engineering. In addition, the proposed approach is also validated experimentally, including not only the steady-state performance but also the close loop transient response when the system perturbation changes, i.e., when the load connected to the UPS output terminals is modified. In Section II, the system under investigation is presented and the used FCS-MPC strategy is described. Section III provides the prediction model design. The performance of FCS-MPC is evaluated in a UPS laboratory prototype using the proposed and the conventional prediction models in Section IV. The accuracy of the two approaches is compared with the help of experimental results, showing that the proposed prediction model provides a more accurate representation of the output current. In addition, the effect on the FCS-MPC performance is assessed. Finally, the conclusion is drawn in Section V.

II. SYSTEM DESCRIPTION AND FCS-MPC STRATEGY

The system under study consists of a three-phase two-level voltage source inverter (VSI) with an output LC filter and an unknown load connected to the filter. The corresponding electric circuit is shown in Fig. 1. The main variables and parameters that characterize the system are summarized in Table I. In the proposed approach, the measured signals are $i_{f,abc}$ and $v_{o,abc}$, while $i_{o,abc}$ is estimated by the proposed augmented state observer. The control objective is to produce the desired sinusoidal output voltage $v_{o,abc}^*$, independently of the harmonic content of the current drawn by the output load $i_{o,abc}$.

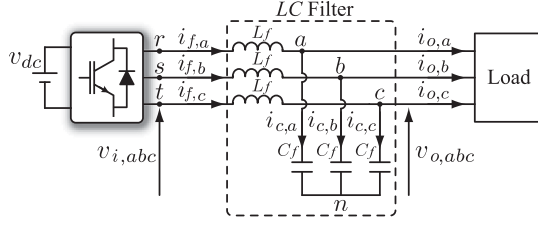


Fig. 1. Electric circuit of the UPS system under study.

TABLE I
SYSTEM VARIABLES AND PARAMETERS

Variable	Description
L_f	Output filter inductor
C_f	Output filter capacitor
$i_{f,abc} = [i_{f,a} \ i_{f,b} \ i_{f,c}]^T$	Output filter inductor current
$v_{o,abc} = [v_{o,a} \ v_{o,b} \ v_{o,c}]^T$	Output filter capacitor voltage
$v_{i,abc} = [v_{i,a} \ v_{i,b} \ v_{i,c}]^T$	VSI output voltage
v_{dc}	DC-link voltage
$S_{abc} = [S_a \ S_b \ S_c]^T$	VSI switching state
$i_{o,abc} = [i_{o,a} \ i_{o,b} \ i_{o,c}]^T$	Output load current
$v_{o,abc}^* = [v_{o,a}^* \ v_{o,b}^* \ v_{o,c}^*]^T$	Output filter capacitor reference voltage
ω	Angular frequency of the reference voltage
f_s	Sampling frequency

A. Original System Model

To analyze the system, the dynamic equations representing the system behavior are expressed in the $\alpha\beta$ stationary reference frame. The controller will be implemented in discrete-time with the sampling frequency f_s . To this end, at each sampling instant k , any system variable $\chi_{abc,k}$ is transformed from abc to the $\alpha\beta$ frame as χ_k^1 by using the well-known power-invariant Clarke transformation. Therefore, $\chi_k = T_{abc}^{\alpha\beta} \chi_{abc,k}$, where

$$T_{abc}^{\alpha\beta} = \sqrt{\frac{2}{3}} \begin{bmatrix} 1 & -\frac{1}{2} & -\frac{1}{2} \\ 0 & \frac{\sqrt{3}}{2} & -\frac{\sqrt{3}}{2} \end{bmatrix}. \quad (1)$$

The discrete-time state space model of the system in the $\alpha\beta$ frame is presented in Table II². The state variables are the filter inductor current and capacitor voltage $i_{f,k}$ and $v_{o,k}$, respectively. The system input is the VSI output voltage $v_{i,k}$. In this representation, the system outputs are equal to the state variables. Also, the so-called process and measurement noises are incorporated into the state space model as ϖ_k and ν_k , respectively. It should be noted that the load current $i_{o,k}$ is considered as an external disturbance. Finally, the discrete-time system model matrices A , B , C , and E can be obtained when a zero order hold approach is applied to the continuous-time plant described in state space form by the matrices A_c , B_c , C_c , and E_c [41].

In this system, the input $v_{i,k}$ can be computed as

$$v_{i,k} = v_{dc,k} T_{abc}^{\alpha\beta} S_{abc,k} \quad (2)$$

¹Note that the subscript $\alpha\beta$ is omitted to allow a more compact notation.

² I_n and O_n represent identity and zero matrices of dimension $n \times n$, respectively.

TABLE II
SPACE STATE SYSTEM DESCRIPTION

State space system	$x_{k+1} = Ax_k + Bu_k + Ei_{o,k} + \varpi_k$
State variables	$x_k^T = [i_{f,k}^T \ v_{o,k}^T]$
System input	$u_k = v_{i,k} = v_{dc,k} T_{abc}^{\alpha\beta} S_{abc,k}$
System output	$y_k^T = [i_{f,k}^T \ v_{o,k}^T]$
Discrete system matrices	$A = e^{A_c T_s}$ $A_c = \begin{bmatrix} O_2 & -\frac{1}{L_f} I_2 \\ \frac{1}{C_f} I_2 & O_2 \end{bmatrix}$ $B = \int_0^{T_s} e^{A_c(T_s-\tau)} B_c d\tau$ $B_c = \begin{bmatrix} \frac{1}{L_f} I_2 \\ O_2 \end{bmatrix}$ $E = \int_0^{T_s} e^{A_c(T_s-\tau)} E_c d\tau$ $E_c = \begin{bmatrix} O_2 \\ -\frac{1}{C_f} I_2 \end{bmatrix}$ $C = I_4$

where $v_{dc,k}$ is the dc-link voltage and $S_{abc,k}$ is the switching state of the inverter at time step k , with $S_j|_{j=a,b,c} \in \{0, 1\}$. Therefore, there exists a finite number of VSI output voltage values determined by the possible switching states of the inverter [7]. This defines the system's finite control set, which motivates one to design an FCS-MPC strategy.

B. FCS-MPC Design

The FCS-MPC objective is to track the desired reference output voltage $v_{o,k}^*$. To achieve this objective, the cost function is designed as

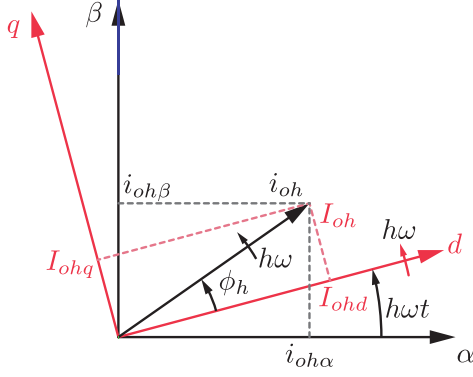
$$g_k = \|v_{o,k+2}^* - v_{o,k+2}\|_2^2 + \lambda \|S_{abc,k+1} - S_{abc,k}\|_2^2. \quad (3)$$

This cost function is composed of two terms. The former one computes the output voltage tracking error at time step $k+2$. This is necessary to avoid the effect of the digital delay, because the control algorithm at time step k computes the control action to be applied at $k+1$. The second term is related to the switching effort and penalizes the number of commutations of the power semiconductors. The relative importance of both terms in the cost function is determined by the weighting factor λ . Higher values of λ increase the switching penalty over the tracking error, resulting in a reduction of the average switching frequency.

Note that according to the state space model in Table II, the output voltage $v_{o,k+2}$ depends on the control input at time step $k+1$, which can be computed using (2) moved by one time step ahead. Therefore, the cost function value only depends on the switching state applied at $k+1$, and the optimal control problem consists of choosing the $S_{abc,k+1}$ that minimizes (3). The optimization algorithm accomplishes this task. In this work, a one-step prediction horizon $N_p = 1$ is considered. Thus, a standard ESA is chosen as the optimization algorithm.

III. PREDICTION MODEL DESIGN

To complete the FCS-MPC design in Section II-B one needs a prediction model to compute the future values of $v_{o,k+2}$ as a function of $S_{abc,k+1}$. If the state space model in Table II is analyzed, the main problem is that the output load current

Fig. 2. General representation of the harmonic vector component i_{oh} .

dynamic is unknown because it depends on the particular load connected to the system. Therefore, to design the prediction model some assumptions have to be made about the behavior of the load.

As a general case, it could be considered that the output current vector in the $\alpha\beta$ frame consists of the sum of different harmonic vector components i_{oh} with $h \in H \in \mathbb{Z}$. The vector i_{oh} rotates at the angular speed $h\omega$ and can be represented in a synchronous reference frame by $I_{oh} \in \mathbb{R}^2$ as shown in Fig. 2, which is a vector that characterizes the amplitude and phase of the h^{th} harmonic vector i_{oh} . Thus, the output current vector can be written as

$$i_o = \sum_{h \in H} i_{oh} = \sum_{h \in H} e^{Jh\omega t} I_{oh} \quad (4)$$

where

$$J = \begin{bmatrix} 0 & -1 \\ 1 & 0 \end{bmatrix} \quad (5)$$

and

$$e^{Jh\omega t} = \begin{bmatrix} \cos(h\omega t) & -\sin(h\omega t) \\ \sin(h\omega t) & \cos(h\omega t) \end{bmatrix} \quad (6)$$

is the rotation matrix [42]. Assuming that the components of I_{oh} are unknown constant or slowly varying signals, it is possible to compute the derivative with respect to time for each individual harmonic component as

$$\frac{di_{oh}}{dt} = Jh\omega e^{Jh\omega t} I_{oh} = Jh\omega i_{oh}. \quad (7)$$

Expressions (4) and (7) allow one to define an augmented state space model in the time domain that takes into account the nature of the load. For instance, if one considers that the load current is composed of the non triple odd harmonics $H = \{1, -5, \dots, m\}$ ³ then, the augmented state vector, the system input and output are defined as

$$x_a = [i_f^T \ v_o^T \ i_{o1}^T \ i_{o5}^T \ \dots \ i_{om}^T]^T \quad (8)$$

$$u = v_i, \ y = [i_f^T \ v_o^T]^T \quad (9)$$

³Note that each particular harmonic is a positive- or negative-sequence vector [43]. For instance, the fifth harmonic component is a negative-sequence vector rotating at -5ω , thus it is represented using $h = -5$.

respectively, leading to the following augmented state space system:

$$\frac{dx_a}{dt} = A_{ac}x_a + B_{ac}u + \varpi \quad (10)$$

$$y = C_{ac}x_a + \nu \quad (11)$$

in which

$$A_{ac} = \begin{bmatrix} O_2 & -\frac{1}{L_f}I_2 & O_2 & O_2 & \dots & O_2 \\ \frac{1}{C_f}I_2 & O_2 & -\frac{1}{C_f}I_2 & -\frac{1}{C_f}I_2 & \dots & -\frac{1}{C_f}I_2 \\ O_2 & O_2 & J\omega & O_2 & \dots & O_2 \\ O_2 & O_2 & O_2 & -J5\omega & \dots & O_2 \\ \vdots & \vdots & \vdots & \vdots & \ddots & \vdots \\ O_2 & O_2 & O_2 & O_2 & \dots & Jm\omega \end{bmatrix} \quad (12)$$

$$B_{ac} = \begin{bmatrix} \frac{1}{L_f}I_2 \\ O_2 \\ O_2 \\ O_2 \\ \vdots \\ O_2 \end{bmatrix}, \quad C_{ac} = \begin{bmatrix} I_2 & O_2 & O_2 & O_2 & \dots & O_2 \\ O_2 & I_2 & O_2 & O_2 & \dots & O_2 \end{bmatrix} \quad (13)$$

are the continuous time plant matrices, with I_2 and O_2 representing identity and zero matrices of dimension 2×2 , respectively.

This system can be discretized by using the exact Euler discretization method and is proposed to be used as the new prediction model for FCS-MPC as

$$x_{a,k+1} = A_a x_{a,k} + B_a u_k + \varpi_k \quad (14)$$

$$y_k = C_a x_{a,k} + \nu_k \quad (15)$$

where A_a , B_a , and C_a are the resulting matrices after applying the exact Euler discretization method to the continuous-time plant (10), (11). However, to take full advantage of this model, it is required to know all the harmonic components in the load current i_{oh} . Because these values cannot be directly measured, an observer is designed to address this issue. The observer can be formulated in the discrete domain as [45]

$$\hat{x}_{a,k+1} = A_a \hat{x}_{a,k} + B_a u_k + G_{obs} (y_k - \hat{y}_k) \quad (16)$$

$$\hat{y}_k = C_a \hat{x}_{a,k} \quad (17)$$

where $\hat{x}_{a,k}$ and $\hat{x}_{a,k+1}$ are the augmented state estimates at time step k and $k+1$, respectively, u_k represents the augmented system input at time step k and it is calculated as in (2) and \hat{y}_k is the augmented system output estimate at the time step k .

The last step is to design the observer gain matrix G_{obs} so that the closed-loop observer matrix $A_{obs} = A_a - G_{obs}C_a$ is Schur stable.⁴ This can be done considering the observer (16), (17) as a steady-state Kalman filter [41]. Thus, the matrix G_{obs} can be computed as the following Riccati equation:

$$G_{obs} = A_a P C_a^T (C_a P C_a^T + R_f)^{-1} \quad (18a)$$

$$P = A_a P A_a^T - G_{obs} C_a P A_a^T + Q_f \quad (18b)$$

⁴A square matrix $A \in \mathbb{R}^{n \times n}$ is said to be Schur stable if all eigenvalues of A have norm strictly less than one [46].

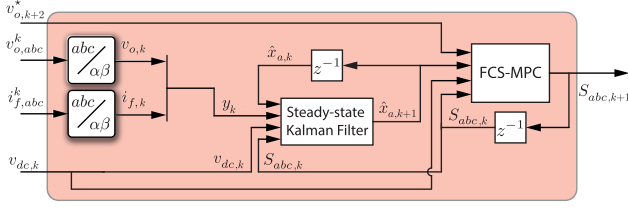


Fig. 3. Block diagram of the proposed control strategy.

where P is the steady-state estimate covariance matrix, and R_f and Q_f denote the measurement and process noise covariance matrices. On one hand, the measurement noise covariance matrix is related to the current and voltage sensor covariance. It is reasonable to assume that all current sensors and voltage sensors have the same covariance r_i and r_v , respectively. These values depend on the experimental setup and can be computed by recording a large number of measurements from each sensor fed with a constant input value and computing the covariance of the data set. Then, the matrix R_f can be defined as

$$R_f = \begin{bmatrix} r_i I_2 & O_2 \\ O_2 & r_v I_2 \end{bmatrix}. \quad (19)$$

On the other hand, the process noise covariance matrix is related to unmodeled or wrongly modeled state dynamics in the state space model. Since the electric model for this circuit does reflect quite well the system dynamics, the process covariance can be chosen as

$$Q_f = q_f I_n \quad (20)$$

where q_f is a small positive scalar value and I_n is the identity matrix with dimension $n \times n$ with n equal to the order of the vector $\hat{x}_{a,k}$. Note that for a given measurement covariance matrix R_f , smaller values of q_f will imply that the system model is almost perfect. Thus, the observer will tend to rely more on predictions rather than measurements. Conversely, larger values of q_f will imply that the observer will rely more on the output measurements. However, this will increase the amount of noise coming from sensors that is transferred to the estimated states. Consequently, this tuning parameter can be used to choose the resulting observer bandwidth. Once R_f and Q_f are defined, inserting (18a) into (18b) allows one to compute P as the solution to the discrete-time algebraic Riccati equation [41]. Once P is computed, G_{obs} can be determined from (18a). Note that P and G_{obs} are time-invariant matrices. Therefore, they can be computed off-line avoiding the increase of the computational burden during real time implementation, e.g., using the *idare* function in MATLAB. Alternatively, an autocovariance least-squares (ALS) method can be used to tune the covariance matrices Q_f and R_f ; see, e.g., [47], [48]. However, an ALS method requires extra calculations since they need to be computed online at each sampling instant.

A block diagram for the proposed control and observer structure is depicted in Fig. 3. At time step k the dc-link voltage and the output filter voltage and current are measured. The system output vector y_k can be calculated by transforming the

TABLE III
PARAMETERS FOR EXPERIMENTS

Parameters	Value
Output filter inductor, L_f	2 mH
Output filter capacitor, C_f	50 μ F
Rectifier filter inductor, L_r	2 mH
Rectifier output capacitor, C_r	2200 μ F
DC load resistor	180 Ω
DC-link voltage, v_{dc}	700 V
Voltage reference (phase to ground)	230 V
Fundamental frequency	50 Hz
Sampling frequency, f_s	40 kHz
Weighting factor, λ	1.5
Kalman filter tuning parameter, q_f	0.0001

variables $v_{o,abc}^k$ and $i_{f,abc}^k$ to the $\alpha\beta$ frame. The system input u_k is defined by the dc-link voltage measurement $v_{dc,k}$ and the optimal switching state $S_{abc,k}$ calculated in the previous iteration of the algorithm which is applied in the current sampling interval. This information is used to compute the augmented state estimate $\hat{x}_{a,k+1}$ by using the proposed augmented state observer (16), (17). Finally, the FCS-MPC determines the optimal control action $S_{abc,k+1}$ for the time step $k+1$ by using the prediction model (14), (15) to compute the output filter voltage prediction values at time step $k+2$ for each possible switching state and minimizing the cost function (3).

IV. EXPERIMENTAL RESULTS

In this section, the effectiveness of the proposed prediction model is verified in the test bench depicted in Fig. 4. Two experimental tests are conducted. The first one investigates the effect of considering a different number of harmonic components in the prediction model when a nonlinear load is connected to the UPS output. The second test compares the system performance when the conventional prediction model in [34] and the proposed one are used to control the output voltage applied to a diode rectifier.

The proposed FCS-MPC is implemented on the Pynq-Z1 evaluation board, which is a Xilinx system on a chip Zynq-7000-based control hardware platform. The system parameters for the experiments are summarized in Table III. The weighting factor λ value is chosen to limit the average switching frequency produced by the FCS-MPC. The value is set heuristically in the experiments in order to achieve an average switching frequency of 5 kHz. In addition, the Kalman filter tuning parameter q_f is designed to provide an observer bandwidth of roughly 1 kHz. Note that the observer bandwidth is computed calculating the natural frequency of the slowest pole of the resulting closed-loop observer matrix A_{obs} . Finally, the output filter inductor current and capacitor voltage sensor covariances are $r_i = 0.0009$ and $r_v = 0.06$, respectively.

A. Assessment of the Proposed Prediction Model Design

The first experimental test evaluates the influence of the number of harmonics considered in the prediction model. The output capacitor voltage, load current, output current estimate



Fig. 4. Test bench: (a) VSI and LC filter, (b) LC filter and voltage and current sensors, (c) nonlinear load and, (d) control hardware and user interface.

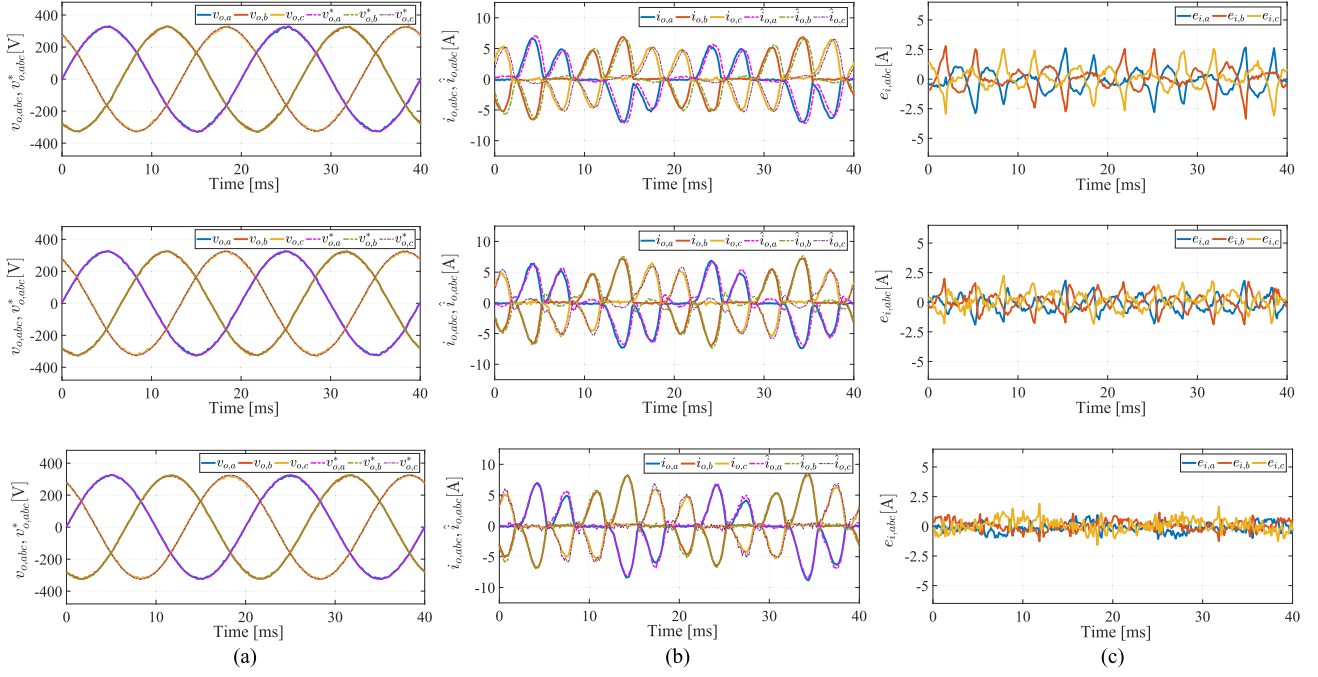


Fig. 5. Output filter capacitor voltage, output load current and current estimation error in the steady-state when the proposed prediction model is used. (a) From top to bottom: output voltage with $H = \{1\}$, $H = \{1, -5\}$ and $H = \{1, -5, 7, -11, 13\}$, (b) from top to bottom: load current with $H = \{1\}$, $H = \{1, -5\}$ and $H = \{1, -5, 7, -11, 13\}$ and (c) from top to bottom: current estimation error $e_{i,j} = (i_{o,j} - \hat{i}_{o,j})|_{j=a,b,c}$ with $H = \{1\}$, $H = \{1, -5\}$ and $H = \{1, -5, 7, -11, 13\}$.

waveform, and current estimation error are presented in Fig. 5 for $H = \{1\}$, $H = \{1, -5\}$ and $H = \{1, -5, 7, -11, 13\}$. Increasing the number of harmonics in H provides a more accurate output current estimate. Particularly, the phase shift between the actual and the estimate current is removed, allowing the observer to properly track the actual load current. Improving the observer accuracy allows FCS-MPC to increase its performance. This statement is confirmed when the total harmonic distortion (THD) and the harmonic spectrum of the output capacitor voltage are analyzed. Fig. 6 shows how these characteristics change as the number of harmonics in H increases. Clearly, FCS-MPC is able to compensate a particular harmonic when such harmonic order is included in the observer. Based on these results, it is also concluded that low order harmonics have more influence on the observer performance than high order ones. In addition, experiments show that when a low order harmonic is included in the observer not only this particular harmonic is compensated but also the high order ones. For instance, Fig. 6 shows that when $H = \{1, -5\}$ the 11th and 13th harmonic content are smaller

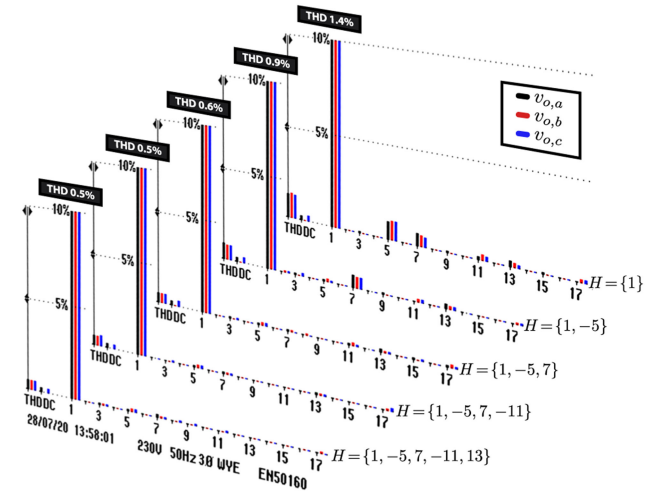


Fig. 6. Output voltage harmonic spectrum for different number of harmonic components in the prediction model.

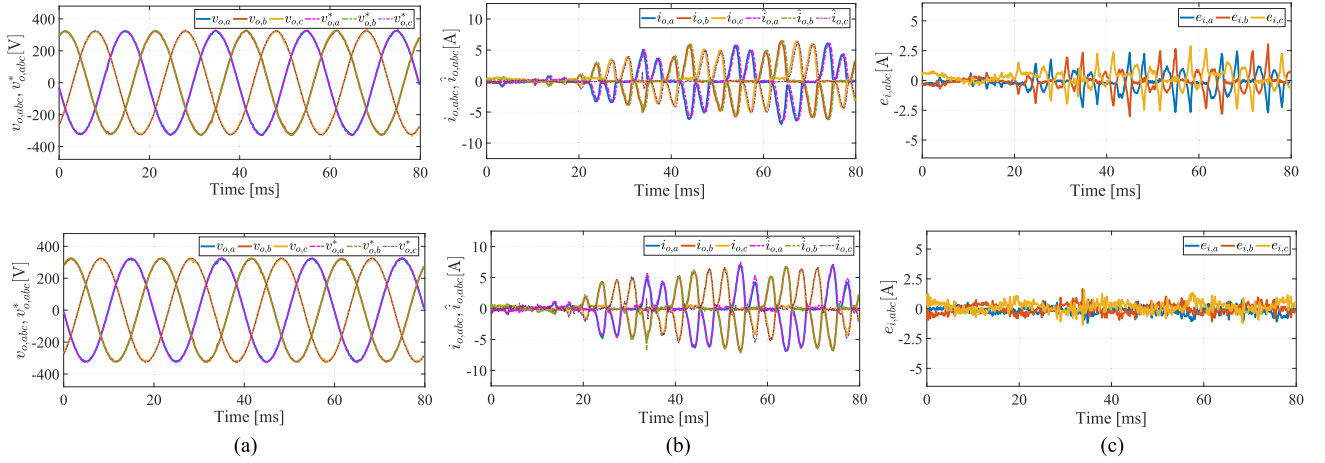


Fig. 7. Output filter capacitor voltage, output load current and current estimation error. Top represents transient response when the conventional prediction model [34] is used and, bottom shows transient result when the proposed prediction model is employed with $H = \{1, -5, 7, -11, 13\}$. (a) Output voltage, (b) load current, and (c) current estimation error.

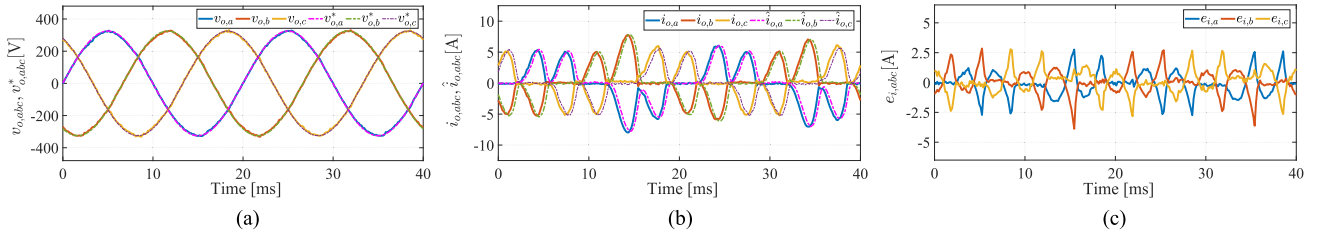


Fig. 8. Output filter capacitor voltage and output load current in the steady-state when the conventional prediction model [34] is used. (a) Output voltage, (b) load current, and (c) current estimation error.

compared to the case $H = \{1\}$. The additional information about the low order harmonic content of the output current provided by the observer reduces FCS-MPC control effort needed to compensate its effect, allowing FCS-MPC to focus on the higher order components. Therefore, as higher order harmonic content is small in general, a limited number of harmonics in H is enough to provide a good closed-loop performance. This is particularly important to limit the computational burden of the algorithm. It is important to highlight that the average switching frequency is 5 kHz in all the experiments independently of the number of harmonics in H . Therefore, the system performance is improved without increasing the switching losses.

B. Conventional Versus Proposed Prediction Model

Once the performance of the proposed model is assessed, it is convenient to compare its performance against the conventional solution. The most common approach to estimate the output load current is to assume that $i_{o,k+1} = i_{o,k}$ [34]. To assess the controller performance both the transient and the steady-state responses are evaluated. Fig. 7 shows the transient response for both prediction model approaches when the load is suddenly connected to the UPS output terminals. The comparison of both performances allows one to conclude that the proposed observer maintains the dynamic response compared to the conventional

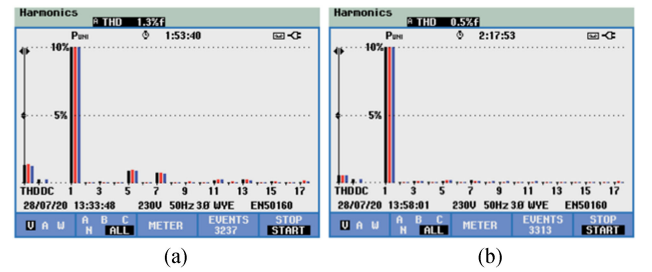


Fig. 9. Spectrum of the output voltage. (a) Conventional prediction model [34] and (b) proposed prediction model $H = \{1, -5, 7, -11, 13\}$.

solution. Fig. 8 shows the output capacitor voltage, load current, output current estimate, and current estimation error at steady-state for the conventional solution. This observer provides a good estimate but the phase shift between the actual and the estimated current is noticeable. As a consequence, FCS-MPC is not able to compensate the effect of the low order harmonic components in the output current. This affects to the harmonic spectrum of the output capacitor voltage, where these low order harmonics are present in Fig. 9(a). Clearly, the harmonic spectrum in Fig. 9(b) when the proposed prediction model is used with $H = \{1, -5, 7, -11, 13\}$ is better. In addition, the proposed prediction model reduces the THD from 1.3% to

0.5%. Finally, the computational cost for both controllers are measured in the control hardware. The conventional solution needs 12.62 μs to complete the algorithm computation while the proposed approach takes 14.99 μs , which is not a significant difference for the current state-of-the-art control hardware platforms. Therefore, it can be concluded that the new proposal performs better than the conventional solution.

V. CONCLUSION

This article studies the influence an observer-based prediction model has on the closed-loop performance of an FCS-MPC strategy governing a UPS system. This problem is challenging due to the lack of information about the load connected to the UPS output terminals. Conventional solution relies on the fact that FCS-MPC uses a high sampling frequency, assuming thus that the output current is almost constant from one sampling instant to the next one. Experimental results show that with this approach FCS-MPC only compensates high order harmonic components in the load, but does not properly take care of low order harmonics due to the lack of this information in the prediction model. In contrast, in this article it is proposed to consider the fact that the load current is a periodical signal, which is composed of the sum of different harmonics, to design the prediction model. This key idea is used to develop a steady-state Kalman filter to estimate the output current, providing the low order harmonic content information of the output load to the prediction model. Experimental results show that this new approach allows FCS-MPC to compensate not only high but also low order harmonic components in the load when they are included in the model. These results also show that due to the ability of FCS-MPC to compensate high order harmonic content, it is not necessary to include a large number of harmonics in the prediction model to achieve a high performance. This is particularly important to limit the computational burden of the algorithm. In addition, the proposed prediction model does not modify the average switching frequency of FCS-MPC. Thus, performance is improved while keeping the switching losses in the same range. Finally, the comparative experimental results for the proposed and conventional solutions allow one to conclude that the proposed approach is more suitable for a UPS application than the conventional one. Improving the accuracy of the output load estimate increases the system performance by lowering the THD of the generated output voltage, which is reduced from 1.3% to 0.5%, i.e., by 61.5%.

Future research direction should address the use of different approaches to deal with parameter and load uncertainties, like model-free FCS-MPC (MF-FCS-MPC) for UPS system. MF-FCS-MPC based on system identification methods or difference detection techniques have shown promising results for other applications. Therefore, studies should investigate both alternatives. Besides the controller design, robustness and stability for this approach should be analyzed in detail for the UPS application, where the resonant frequency of the output LC filter can produce instabilities in the system.

REFERENCES

- [1] S. Kouro, P. Cortes, R. Vargas, U. Ammann, and J. Rodriguez, "Model predictive control: a simple and powerful method to control power converters," *IEEE Trans. Ind. Electron.*, vol. 56, no. 6, pp. 1826–1838, Jun. 2009.
- [2] S. Vazquez *et al.*, "Model predictive control: A review of its applications in power electronics," *IEEE Ind. Electron. Mag.*, vol. 8, no. 1, pp. 16–31, Mar. 2014.
- [3] S. Vazquez, J. Rodriguez, M. Rivera, L. G. Franquelo, and M. Norambuena, "Model predictive control for power converters and drives: Advances and trends," *IEEE Trans. Ind. Electron.*, vol. 64, no. 2, pp. 935–947, Feb. 2017.
- [4] T. Dragicevic, S. Vazquez, and P. Wheeler, "Advanced control methods for power converters in DG systems and microgrids," *IEEE Trans. Ind. Electron.*, vol. 68, no. 7, pp. 5847–5862, Jul. 2021.
- [5] P. Karamanakos, T. Geyer, and R. Kennel, "On the choice of norm in finite control set model predictive control," *IEEE Trans. Power Electron.*, vol. 33, no. 8, pp. 7105–7117, Aug. 2018.
- [6] P. Karamanakos and T. Geyer, "Guidelines for the design of finite control set model predictive controllers," *IEEE Trans. Power Electron.*, vol. 35, no. 7, pp. 7434–7450, Jul. 2020.
- [7] P. Cortes *et al.*, "Guidelines for weighting factors design in model predictive control of power converters and drives," in *Proc. IEEE Int. Conf. Ind. Technol.*, 2009, pp. 1–7.
- [8] J. Rodriguez *et al.*, "State of the art of finite control set model predictive control in power electronics," *IEEE Trans. Ind. Inform.*, vol. 9, no. 2, pp. 1003–1016, May 2013.
- [9] C. Bordons and C. Montero, "Basic principles of MPC for power converters: Bridging the gap between theory and practice," *IEEE Ind. Electron. Mag.*, vol. 9, no. 3, pp. 31–43, Sep. 2015.
- [10] S. Kouro, M. A. Perez, J. Rodriguez, A. M. Llor, and H. A. Young, "Model predictive control: MPC's role in the evolution of power electronics," *IEEE Ind. Electron. Mag.*, vol. 9, no. 4, pp. 8–21, Dec. 2015.
- [11] P. Karamanakos, T. Geyer, N. Oikonomou, F. D. Kieferndorf, and S. Manias, "Direct model predictive control: A review of strategies that achieve long prediction intervals for power electronics," *IEEE Ind. Electron. Mag.*, vol. 8, no. 1, pp. 32–43, Mar. 2014.
- [12] T. Geyer and D. E. Quevedo, "Multistep finite control set model predictive control for power electronics," *IEEE Trans. Power Electron.*, vol. 29, no. 12, pp. 6836–6846, Dec. 2014.
- [13] P. Acuna, C. A. Rojas, R. Baidya, R. P. Aguilera, and J. E. Fletcher, "On the impact of transients on multistep model predictive control for medium-voltage drives," *IEEE Trans. Power Electron.*, vol. 34, no. 9, pp. 8342–8355, Sep. 2019.
- [14] T. Geyer, G. Papafotiou, and M. Morari, "Model predictive direct torque control-part i: Concept, algorithm, and analysis," *IEEE Trans. Ind. Electron.*, vol. 56, no. 6, pp. 1894–1905, Jun. 2009.
- [15] H. Miranda, P. Cortes, J. I. Yuz, and J. Rodriguez, "Predictive torque control of induction machines based on state-space models," *IEEE Trans. Ind. Electron.*, vol. 56, no. 6, pp. 1916–1924, Jun. 2009.
- [16] C. A. Rojas, J. I. Yuz, C. A. Silva, and J. Rodriguez, "Comments on "predictive torque control of induction machines based on state-space models"," *IEEE Trans. Ind. Electron.*, vol. 61, no. 3, pp. 1635–1638, Mar. 2014.
- [17] M. Preindl and S. Bolognani, "Model predictive direct torque control with finite control set for PMSM drive systems, part 2: Field weakening operation," *IEEE Trans. Ind. Inform.*, vol. 9, no. 2, pp. 648–657, May 2013.
- [18] M. Preindl and S. Bolognani, "Model predictive direct torque control with finite control set for PMSM drive systems, part 1: Maximum torque per ampere operation," *IEEE Trans. Ind. Inform.*, vol. 9, no. 4, pp. 1912–1921, Nov. 2013.
- [19] S. Vazquez, A. Marquez, R. Aguilera, D. Quevedo, J. I. Leon, and L. G. Franquelo, "Predictive optimal switching sequence direct power control for grid-connected power converters," *IEEE Trans. Ind. Electron.*, vol. 62, no. 4, pp. 2010–2020, Apr. 2015.
- [20] S. Vazquez, P. Acuna, R. P. Aguilera, J. Pou, J. I. Leon, and L. G. Franquelo, "Dc-link voltage-balancing strategy based on optimal switching sequence model predictive control for single-phase H-NPC converters," *IEEE Trans. Ind. Electron.*, vol. 67, no. 9, pp. 7410–7420, Sep. 2020.
- [21] H. Miranda, R. Teodorescu, P. Rodriguez, and L. Helle, "Model predictive current control for high-power grid-connected converters with output LCL filter," in *Proc. 35th Annu. Conf. IEEE Ind. Electron.*, 2009, pp. 633–638.
- [22] N. Panten, N. Hoffmann, and F. W. Fuchs, "Finite control set model predictive current control for grid-connected voltage-source converters with LCL filters: A study based on different state feedbacks," *IEEE Trans. Power Electron.*, vol. 31, no. 7, pp. 5189–5200, Jul. 2016.

- [23] S. A. Davari, D. A. Khaburi, F. Wang, and R. M. Kennel, "Using full order and reduced order observers for robust sensorless predictive torque control of induction motors," *IEEE Trans. Power Electron.*, vol. 27, no. 7, pp. 3424–3433, Jul. 2012.
- [24] J. Wang, F. Wang, Z. Zhang, S. Li, and J. Rodríguez, "Design and implementation of disturbance compensation-based enhanced robust finite control set predictive torque control for induction motor systems," *IEEE Trans. Ind. Inform.*, vol. 13, no. 5, pp. 2645–2656, Oct. 2017.
- [25] L. Yan, F. Wang, M. Dou, Z. Zhang, R. Kennel, and J. Rodríguez, "Active disturbance-rejection-based speed control in model predictive control for induction machines," *IEEE Trans. Ind. Electron.*, vol. 67, no. 4, pp. 2574–2584, Apr. 2020.
- [26] C. Xia, M. Wang, Z. Song, and T. Liu, "Robust model predictive current control of three-phase voltage source PWM rectifier with online disturbance observation," *IEEE Trans. Ind. Inform.*, vol. 8, no. 3, pp. 459–471, Aug. 2012.
- [27] Z. Song, C. Xia, and T. Liu, "Predictive current control of three-phase grid-connected converters with constant switching frequency for wind energy systems," *IEEE Trans. Ind. Electron.*, vol. 60, no. 6, pp. 2451–2464, Jun. 2013.
- [28] Y. Zhang, J. Jin, and L. Huang, "Model-free predictive current control of pmsm drives based on extended state observer using ultralocal model," *IEEE Trans. Ind. Electron.*, vol. 68, no. 2, pp. 993–1003, Feb. 2021.
- [29] J. Rodríguez, R. Heydari, Z. Rafiee, H. A. Young, F. Flores-Bahamonde, and M. Shahparasti, "Model-free predictive current control of a voltage source inverter," *IEEE Access*, vol. 8, pp. 211104–211114, 2020.
- [30] S. Sabzevari, R. Heydari, M. Mohiti, M. Savaghebi, and J. Rodriguez, "Model-free neural network-based predictive control for robust operation of power converters," *Energies*, vol. 14, no. 8, 2021, Art. no. 2325. [Online]. Available: <https://www.mdpi.com/1996-1073/14/8/2325>
- [31] C.-K. Lin, T.-H. Liu, J.-t. Yu, L.-C. Fu, and C.-F. Hsiao, "Model-free predictive current control for interior permanent-magnet synchronous motor drives based on current difference detection technique," *IEEE Trans. Ind. Electron.*, vol. 61, no. 2, pp. 667–681, Feb. 2014.
- [32] Y. Zhang and J. Liu, "An improved model-free predictive current control of PWM rectifiers," in *Proc. 20th Int. Conf. Elect. Mach. Syst.*, 2017, pp. 1–5.
- [33] V.-T. Le and H.-H. Lee, "An enhanced model-free predictive control to eliminate stagnant current variation update for PWM rectifiers," *IEEE Trans. Emerg. Sel. Topics Power Electron.*, to be published, doi: [10.1109/JESTPE.2021.3058737](https://doi.org/10.1109/JESTPE.2021.3058737).
- [34] P. Cortes, G. Ortiz, J. I. Yuz, J. Rodríguez, S. Vazquez, and L. G. Franquelo, "Model predictive control of an inverter with output LC filter for UPS applications," *IEEE Trans. Ind. Electron.*, vol. 56, no. 6, pp. 1875–1883, Jun. 2009.
- [35] T. Dragičević and M. Novak, "Weighting factor design in model predictive control of power electronic converters: An artificial neural network approach," *IEEE Trans. Ind. Electron.*, vol. 66, no. 11, pp. 8870–8880, Nov. 2019.
- [36] P. Mattavelli, "An improved deadbeat control for ups using disturbance observers," *IEEE Trans. Ind. Electron.*, vol. 52, no. 1, pp. 206–212, Feb. 2005.
- [37] S. Vazquez, A. Marquez, J. I. Leon, L. G. Franquelo, and T. Geyer, "FCS-MPC and observer design for a VSI with output LC filter and sinusoidal output currents," in *Proc. 11th IEEE Int. Conf. Compat., Power Electron. Power Eng.*, 2017, pp. 677–682.
- [38] E. Zafra *et al.*, "Finite control set model predictive control with an output current observer in the dq-synchronous reference frame for an uninterruptible power supply system," in *Proc. IEEE 13th Int. Conf. Compat., Power Electron. Power Eng.*, 2019, pp. 1–6.
- [39] C. Fischer, S. Mariéthoz, and M. Morari, "A model predictive control approach to reducing low order harmonics in grid inverters with LCL filters," in *Proc. 39th Annu. Conf. IEEE Ind. Electron. Soc.*, 2013, pp. 3252–3257.
- [40] B. Majmunović, T. Dragičević, and F. Blaabjerg, "Multi objective modulated model predictive control of stand-alone voltage source converters," *IEEE Trans. Emerg. Sel. Topics Power Electron.*, vol. 8, no. 3, pp. 2559–2571, Sep. 2020.
- [41] G. C. Goodwin, S. F. Graebe, and M. E. Salgado, *Control System Design*, P. Hall, Ed., Upper Saddle River, New Jersey, USA: Pearson, 2001.
- [42] G. Escobar, A. M. Stankovic, and P. Mattavelli, "An adaptive controller in stationary reference frame for D-statcom in unbalanced operation," *IEEE Trans. Ind. Electron.*, vol. 51, no. 2, pp. 401–409, Apr. 2004.
- [43] S. Vazquez, J. A. Sanchez, M. R. Reyes, J. I. Leon, and J. M. Carrasco, "Adaptive vectorial filter for grid synchronization of power converters under unbalanced and/or distorted grid conditions," *IEEE Trans. Ind. Electron.*, vol. 61, no. 3, pp. 1355–1367, Mar. 2014.
- [44] B. D. O. Anderson and J. B. Moore, *Optimal Filtering*. Englewood Cliffs, NJ, USA: Prentice-Hall, 1979.
- [45] G. Ellis, *Observers in Control Systems: A Practical Guide*. New York, NY, USA: Academic, 2002.
- [46] R. Bhatia, *Matrix Analysis, 1st ed.*, (Series 169). New York, NY, USA: Springer-Verlag, 1997.
- [47] B. J. Odelson, M. R. Rajamani, and J. B. Rawlings, "A new autocovariance least-squares method for estimating noise covariances," *Automatica*, vol. 42, no. 2, pp. 303–308, 2006.
- [48] J. Rodas, C. Martín, M. R. Arahal, F. Barrero, and R. Gregor, "Influence of covariance-based ALS methods in the performance of predictive controllers with rotor current estimation," *IEEE Trans. Ind. Electron.*, vol. 64, no. 4, pp. 2602–2607, Apr. 2017.



Sergio Vazquez (Fellow, IEEE) was born in Seville, Spain, in 1974. He received the M.S. and Ph.D. degrees in industrial engineering from the University of Seville (US), Seville, Spain, in 2006, and 2010, respectively.

Since 2002, he is with the Power Electronics Group working in R&D projects. He is an Associate Professor with the Department of Electronic Engineering, US. His research interests include power electronics systems, modeling, modulation, and control of power electronics converters applied to renewable energy

technologies.

Dr. Vazquez was recipient as coauthor of the 2012 Best Paper Award of the IEEE TRANSACTIONS ON INDUSTRIAL ELECTRONICS and 2015 Best Paper Award of the *IEEE Industrial Electronics Magazine*. He is involved in the Energy Storage Technical Committee of the IEEE Industrial Electronics Society and is currently serving as an Associate Editor of the IEEE TRANSACTIONS ON INDUSTRIAL ELECTRONICS.



Eduardo Zafra (Graduate Student Member, IEEE) was born in Seville, Spain, in 1994. He received the B.S. and M.S. degrees in industrial engineering in 2016 and 2019, respectively, from the University of Seville (US), Seville, Spain, where he is currently working toward the Ph.D. degree in automatics, electronics, and telecommunications.

In 2018, he joined the Electronic Engineering Department, Universidad de Sevilla, as a Predoctoral Researcher. His main research interests include control and modulation of power converters and drives, model predictive control, and design for digital embedded systems.



Ricardo P. Aguilera (Member, IEEE) received the B.Sc. degree in electrical engineering from the Universidad de Antofagasta, Antofagasta, Chile, in 2003, the M.Sc. degree in electronics engineering from the Universidad Tecnica Federico Santa Maria, Valparaíso, Chile, in 2007, and the Ph.D. degree in electrical engineering from The University of Newcastle (UoN), Newcastle, NSW, Australia, in 2012.

From 2012 to 2013, he was a Research Academic with UoN, where he was part of the Centre for Complex Dynamic Systems and Control. From 2014 to 2016, he was a Senior Research Associate with The University of New South Wales, Sydney NSW, Australia, where he was part of the Australian Energy Research Institute. Since September 2016, he has been with the School of Electrical and Data Engineering, University of Technology Sydney, Ultimo, NSW, Australia, where he currently holds a Senior Lecturer position. His main research interests include theoretical and practical aspects on model predictive control with application to power electronics, renewable energy integration, and microgrids.



Tobias Geyer (Senior Member, IEEE) received the Dipl.-Ing. and Ph.D. degrees in electrical engineering from ETH Zurich, Zurich, Switzerland, in 2000 and 2005, respectively, and the Habilitation degree in power electronics from ETH Zurich, Zurich, Switzerland, in 2017.

After the Ph.D., he spent three years with GE Global Research, Munich, Germany, three years with the University of Auckland, Auckland, New Zealand, and eight years with ABB's Corporate Research Centre, Baden-Dättwil, Switzerland. There, in 2016, he became a Senior Principal Scientist for power conversion control. He was appointed as an extraordinary Professor with Stellenbosch University, Stellenbosch, South Africa, from 2017 to 2023. In 2020, he joined ABB's medium-voltage drives business as R&D platform Manager of the ACS6000/6080. He is the author of 35 patent families and the book *"Model predictive control of high power converters and industrial drives"* (Hoboken, NJ, USA: Wiley, 2016). He teaches a regular course on model predictive control with ETH Zurich. His research interests include medium-voltage and low-voltage drives, utility-scale power converters, optimized pulse patterns, and model predictive control.

Dr. Geyer was the recipient of the Semikron Innovation Award and the Nagamori Award, both in 2021. He is also the recipient of the 2017 First Place Prize Paper Award in the Transactions on Power Electronics, the 2014 Third Place Prize Paper Award in the Transactions on Industry Applications, and of two Prize Paper Awards at conferences. He is a former Associate Editor for the TRANSACTIONS ON INDUSTRY APPLICATIONS (from 2011 until 2014) and the TRANSACTIONS ON POWER ELECTRONICS (from 2013 until 2019). He was an international program committee vice chair of the IFAC conference on Nonlinear Model Predictive Control in Madison, WI, USA, in 2018. He is a Distinguished Lecturer of the Power Electronics Society in 2020 and 2021.



Jose I. Leon (Fellow, IEEE) was born in Cadiz, Spain. He received the B.S., M.S., and Ph.D. degrees in telecommunications engineering from Universidad de Sevilla (US), Seville, Spain, in 1999, 2001, and 2006, respectively.

He is an Associate Professor with the Department of Electronic Engineering, US. Since 2019, he is also a Chair Professor with the Department of Control Science and Engineering, Harbin Institute of Technology, Harbin, China.

His research interests include modulation and control of power converters for high-power applications and renewable energy systems.

Dr. Leon was a co-recipient of the 2008 Best Paper Award of IEEE Industrial Electronics Magazine, the 2012 Best Paper Award of the IEEE Transactions on Industrial Electronics, and the 2015 Best Paper Award of IEEE Industrial Electronics Magazine. He was the recipient of the 2014 IEEE J. David Irwin Industrial Electronics Society Early Career Award, the 2017 IEEE Bimal K. Bose Energy Systems Award, and the 2017 Manuel Losada Villasante Award for excellence in research and innovation. In 2017, he was elevated to the IEEE fellow grade with the following citation "for contributions to high-power electronic converters."



Leopoldo G. Franquelo (Life Fellow, IEEE) was born in Málaga, Spain. He received the M.Sc. and Ph.D. degrees in electrical engineering from the Universidad de Sevilla, Seville, Spain, in 1977 and 1980, respectively.

From 1982 to 1986, he was an Associate Professor with the Electronics Engineering Department, Sevilla University, Seville, Spain, where he is currently a Professor with the Electronics Engineering Department, since 1986, and a 1000 Talent Professor with the Department of Control Science and Engineering, Harbin Institute of Technology, Harbin, China, since 2016. He has participated in more than 100 Industrial and R&D projects and has authored or coauthored more than 300 papers, 76 of them in IEEE Journals. His current research interests include modulation techniques for multilevel inverters and application to power electronic systems for renewable energy systems.

Dr. Franquelo is an IEEE Industrial Electronics Society (IES) Distinguished Lecturer since 2006. In the IEEE TRANSACTIONS ON INDUSTRY APPLICATIONS, he became an Associate Editor in 2007, Co-Editor-in-Chief in 2014, and the Editor-in-Chief in 2016. He was a Member-at-Large of the IES AdCom from 2002 to 2003, Vice President for Conferences from 2004 to 2007, and President Elect of the IES from 2008 to 2009. He was the President of the IES from 2010 to 2011 and is an IES AdCom Life member. In 2009 and 2013, he received the prestigious Andalusian Research Award and FAMA Award recognizing the excellence of his research career. He has received a number of Best Paper Awards from IEEE journals. In 2012 and 2015, he was the recipient of the Eugene Mittelmann Outstanding Research Achievement Award and the Anthony J. Hornfeck Service Award from IEEE-IES, respectively.